Twenty-five-year Lower tropospheric ozone in subtropical East Asia influenced by climate and emission

Tao Wang*, Jianing Dai, Ka Se Lam, Chun Nan Poon, Guy P. Brasseur

Department of Civil and Environmental Engineering, The Hong Kong Polytechnic University, Hong Kong, China

*Correspondence to: Tao Wang, E-mail: cetwang@polyu.edu.hk

Abstract. Tropospheric ozone affects the earth's radiative balance, oxidative capacity and air quality, yet the long-term ozone trend in East Asia and its driver(s) remain poorly understood. Here we present ozone measurements obtained during 1994-2018 on China's southern coast. The measurement location intercepts China's outflow most of the time and the inflow of tropical maritime air during summer. We found an overall increase in the ozone level (0.35 ppbv $year^{-1}$), and the increase occurred mainly during the first half of the 25-year period but appeared to level off in recent years in Chinese outflow. Large ozone increase (~20% $decade^{-1}$) was found in maritime air. Model simulations show that recent weather conditions have reduced maritime ozone, counteracting the forcing from the growing Southeast Asia's emissions. Our results fill the gap in the long-term ozone trend in Asia and highlight the complex interaction of climate and emission in driving the ozone change.

Plain Language Summary. Tropospheric ozone has great influence on environmental issues ranging from air quality, ecosystem productivity and climate warming. Assessing the ozone impacts in fast-developing Asia has been hindered by the lacking of continuous and long-term measurements. We present here the longest continuous record of surface ozone in non-urban areas of subtropical Asia. Using comprehensive tools, we reveal that the measurements on the south China's coast detected different ozone trends in air from eastern China (increasing in early years but stabilizing lately) and from Southeast Asia (continuous rise and at the largest rate). The latter finding is particularly striking, and we show that climate change actually counteracted the forcing from emission increases from Southeast Asia. Our results fill the gap in the long-term ozone trends in Asia and highlight the complex interaction of climate and emission in driving the ozone trend.

Key points.

- We present the first long-term measurements of background ozone and CO in

subtropical East Asia, which shows an overall ozone increase rate of 0.35 ppbv year^{-1}.

- The ozone increase occurred during the first half of the 25-year period but appeared to level off during recent years in China's outflow.
- Maritime air has shown the largest rate of ozone increase, and climate change has counteracted the forcing from the growing Southeast Asia's emissions.

1. Introduction

Tropospheric ozone is a greenhouse gas that contributes directly to climate warming (Pachauri et al. 2014). It is the major source of hydroxyl radicals that determine the removal rates of many chemically and radiatively active gases in the atmosphere (Warneck 1999). High concentrations of ozone at the ground level have adverse effects on human health and vegetation (Council 1992). The tropospheric ozone burden is influenced by emissions of ozone precursors – oxides of nitrogen (NO_x), carbon monoxide (CO) and volatile organic compounds (VOCs) – and by meteorological conditions that affect the emission and chemistry of the precursors and atmospheric transport patterns (Monks et al. 2015; Jacob and Winner 2009). Ozone levels in urban and rural areas in North America and Europe have mostly decreased in recent decades due to reductions in anthropogenic emissions (Parrish et al. 2014; Gaudel et al. 2018; Akimoto 2003), but the trend and drivers in some regions are quite complicated. Despite the decreases in the regional emission of ozone precursors, the ozone levels in rural areas of the western United States have shown upward trends (Lin et al. 2017), which are attributed to increases in Asian emissions (Lin et al. 2017; Jacob, Logan, and Murti 1999; Cooper et al. 2010), increased frequency of biomass burning (Westerling et al. 2006; Jaffe et al. 2008; Lin et al. 2017) and strengthened downward transport from the stratosphere (Neu et al. 2014; Lin et al. 2015). The tropospheric ozone in the remote central Pacific Ocean is strongly affected by the decadal changes in atmospheric circulation, which weakens the impact of Asian emissions during the spring but enhances it during autumn (Lin et al. 2014). Springtime ozone at Mt Happo, Japan has been suppressed by reduced long-range transport from China in recent years (Okamoto et al. 2018). A modelling study suggested that the trend of shifting ozone precursor emissions to low-latitude regions of Asia has significantly affected the global distribution and burden of tropospheric ozone (Zhang et al. 2016). The tropical and subtropical regions of East Asia are strongly influenced by the monsoon climate and have seen rapid industrialisation in China and Southeast Asian countries over the past 30 years. Here we report surface ozone and carbon monoxide (CO), an ozone precursor and pollution tracer, measured from 1994 to 2018 at Hok

Tsui (HT), a background site on China's south coast, in Hong Kong. These data represent the longest record of surface ozone and CO in this important region of Asia and provide a critical dataset to assess the impact of ozone on the climate and ecosystem. We examined the 25-year ozone change in all four seasons and in major air masses and also compare the data with ozonesonde. We focused on the surprisingly large concentration increase in maritime ozone during summer and used large-scale meteorological and satellite-derived chemical data and a regional chemistry transport model to assess the impact of climate change and emissions on marine ozone.

2. Methods

2.1. Observations and trend analysis

Ozone and carbon monoxide were measured at a coastal background site (HT) by the research team of the Hong Kong Polytechnic University with the ultraviolet absorption and infrared absorption techniques, respectively. The data for 1994-2007 were reported by Wang et al. (2009), to which the reader is referred for a detailed description of the site and data quality control. Ozonesonde was launched by the Hong Kong Observatory at King's Park in the centre of urban Kowloon since 1993, initially on a monthly basis, with the frequency increased to weekly in 1993-1994 and 2000-2001 and after April 2003 (http://www.weather.gov.hk/publica/reprint/r1173.pdf). The ozonesonde data are accessible at the World Ozone and Ultraviolet Radiation Center (http://woudc.org/data/stations/id=344).

To determine the magnitude of the trend's direction, we adopted the nonparametric Theil-Sen (T-S) estimator(Sen 1968) and the Mann-Kendall (M-K) test (Mann 1945) because they do not require prior assumptions of statistical distribution for the data and are resistant to outliers (Lefohn et al. 2017). The T-S estimator was used to compute the rate of change, and the M-K test was used to determine the level of significance. We computed the linear trend for annual and seasonal means and according to air mass groups. For the surface ozone, we also computed the trend for each 5-ppb concentration bin and the non-linear trend for the annual data. For p values greater than 0.05, the exact values are given because they may still have statistical significance (Wasserstein, Schirm, and Lazar 2019). Only the mean values with more than 50% of the data available in a period (i.e., annual and seasonal, air groups) were used for trend analysis.

2.2. Backward trajectories classification

Ten-day backward trajectories were calculated for each hour during 1994-2018 using the Hybrid Single-Particle Lagrangian Integrated Trajectory (HYSPLIT) model (https://www.ready.noaa.gov/hyreg/HYSPLIT_linux.php) driven by 6-hourly Air Resources Laboratory (ARL) FNL archive data with a resolution of 190 km (ftp://arlftp.arlhq.noaa.gov/pub/archives/reanalysis/). The endpoint of the trajectories was 300 m above ground level at HT, which is in the middle of the marine boundary layer. Classification analysis was then used to group trajectories into four main clusters ('Eastern China', 'Aged continental', 'Central China + PRD' and 'Marine') based on the source of the region (Wang et. al., 2009).

2.3. Meteorological and satellite data

The National Center for Atmospheric Prediction and National Center for Atmospheric Research (NCEP/NCAR) global reanalysis data (https://rda.ucar.edu/datasets/ds090.0/) were used to analyse long-term trends and yearly variations in meteorological variables (temperature, solar radiation, relative humidity and precipitation) in Southeast Asia including the South China Sea (0-25 °N; 100-120 °E) for period of June through August.

Satellite data were used to examine the long-term trend of the tropospheric NO_2 and formaldehyde column concentrations as indicators of changes in ozone precursors in Southeast Asia. The formaldehyde column data (http://h2co.aeronomie.be/) were obtained from GOME for the 1997–2002 periods, SCIAMACHY for 2003-2004 and OMI for 2005-2016 (De Smedt et al. 2008; De Smedt et al. 2012). The OMI data were adjusted by multiplying by a factor of 1.25 to correct the systematic difference between OMI and SCIAMCHY (De Smedt et al. 2015). The NO_2 column data were obtained from OMI (http://www.temis.nl/airpollution/no2.html) for 1997-2017 (Boersma et al. 2011). The NO_2 and formaldehyde column concentrations in land and sea mask were separated according to the 'landcover' parameter in the NCEP/NCAR reanalysis data.

2.4. Chemical transport model simulations

Six simulations were conducted with a modified WRF-Chem (v3.6.1) (https://www2.acom.ucar.edu/wrf-chem) with 27×27 km^2 horizontal resolution (Grell et al. 2005; Zhang et al. 2017). The simulations were driven to NCEP/NCAR global reanalysis data in July 1994, 1995,1996, 2016, 2017 and 2018, with the 2016 emission inventory (EI). The outputs from the Model for Ozone and Related Chemical Tracers model were used as the initial

and boundary chemical data. We used the 2016 EI from the Hong Kong Environmental Protection Department for Hong Kong (HKEPD) (https://www.epd.gov.hk/), the 2016 Multi-resolution Emission Inventory for China (MEIC) for the rest of China, MIX for year 2010 for the rest of Asia (http://meicmodel.org/) and the 2012 EDGAR EI for ship emissions (http://edgar.jrc.ec.europa.eu). The emissions are the lower limit for 2016 because land and ship emissions both increased in recent years in Southeast Asia and around the South China Sea.

3. Results

3.1 Ozone and CO trends in the overall data and in different air masses

The yearly mean surface ozone level at HT showed an upward trend during 1994-2018 at rate of 0.35 ppbv year^{-1} (y^{-1}) ($p<0.01$), and the average ozone mixing ratio at 0 to 1 km obtained with ozonesonde during 1994-2017 increased by 0.59 ppbv y^{-1} ($p<0.01$) (Figure 1), which suggests an increase in ozone levels in the entire planetary boundary layer on the South China coast. The increases in surface ozone are mainly in concentrations above 50 ppbv, whilst the mixing ratios below 20 ppbv decreased, which can be explained by increases in NOx emissions (Lefohn et al. 2017). The ozone increase occurred mainly during the early years but appeared to have slowed in the most recent decade (0.62 ppbv y^{-1} in 1994-2006 ($p<0.05$) versus 0.10 ppbv y^{-1} in 2007-2018, $p=0.38$). A polynomial fit gives $[O_3]$ (ppbv) = $29.2 + 0.92 \times t - 0.02 \times t^2$ (at 95% confidence level) (t is year). The increase in surface ozone was seen in all four seasons (0.33 ppbv y^{-1} in spring, 0.50 ppbv y^{-1} in summer, 0.40 ppbv y^{-1} in autumn and 0.36 ppbv yr^{-1} in winter; Figure S1). Particularly interesting was the highest rate of increase in summer, when the south China coast receives the cleanest air of any season. (Indeed, the lowest mean value is found during the summer monsoon season). We further segregated the hourly ozone data according to the four major air masses (Figure 2a). The rate of the ozone increase was 0.36 ppbv y^{-1} in the marine air masses (80% of which are in summer and account for 25.8% of the total trajectories), 0.37 ppbv y^{-1} in 'East China' (32.9% of total trajectories), 0.39 ppbv y^{-1} in 'Central China + PRD (Pearl River Delta)' (11.1% of total trajectories) and 0.34 ppbv y^{-1} in 'Aged continental' (30.1% of the total) ($p<0.01$ in all cases; Figure 2b).

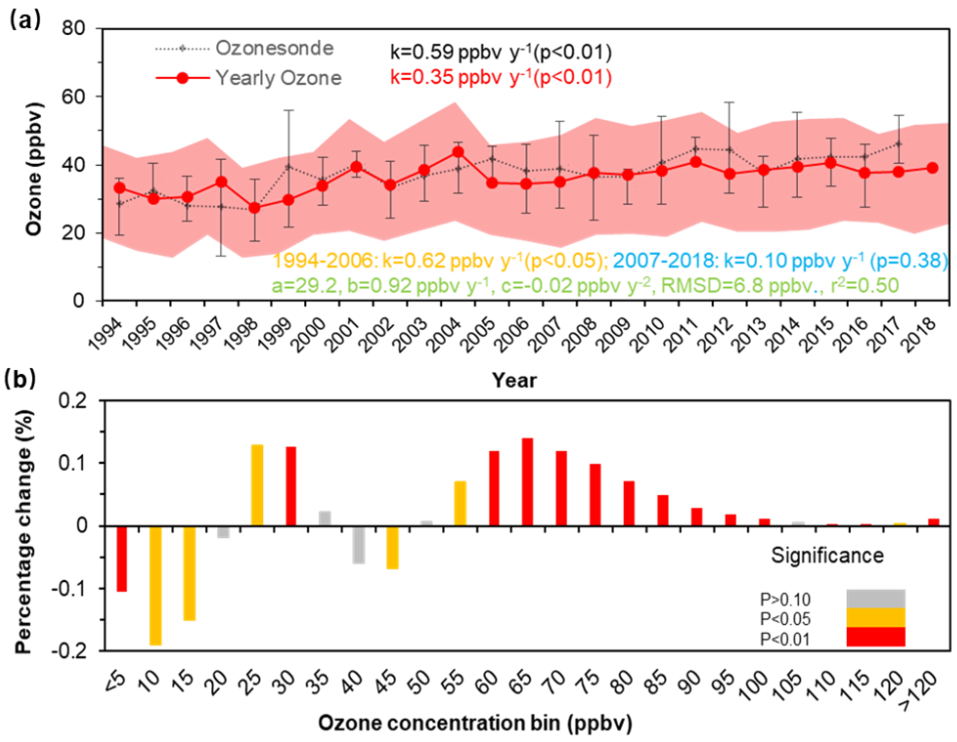

Figure 1. Long-term ozone trend and variability in Hong Kong. (a) Yearly mean surface ozone mixing ratios at Hok Tsui (HT) in 1994-2018 (red) and yearly mixing ratios of ozone at 0 to 1 km from ozonesonde at Kings Park (black) in 1994-2017 (black). Shaded area and vertical bars are 75th and 25th percentiles for hourly surface data and sonde profile, respectively. Also shown are linear fit results for surface ozone (red) and ozonesonde (black) for the entire period and surface ozone for 1994-2006 (yellow) and 2007-2018 (blue). Nonlinear fit of HT data yields $y = a + bx - cx^2$ (with 95% confidence intervals), root-mean-square-deviation (RMSD) of 6.8 ppb and R^2=0.50. (b) Theil-Sen trend of percentage change (% year^{-1}) in each bin of ozone concentration at HT for 1994-2018.

Ozone increases in the air masses that originated on the continent are expected at least until 2011 because the emissions of ozone precursors continued to increase until 2011, when NOx emissions began to decrease but those of VOC continued to increase (Liu et al. 2017; Duncan et al. 2016; De Smedt et al. 2015). Previous studies have shown an increase in ozone in the range of 1 to 2 ppbv y^{-1} during various periods of 1995-2015 at several non-urban sites in East China (Ding et al. 2008; Sun et al. 2016; Ma et al. 2016). We previously reported an increase in surface ozone at HT at a rate of 0.64 to 0.67 ppbv y^{-1} in 1994-2007 in two continental air masses (i.e., 'East China' and 'Central China + PRD') (Wang et al. 2009). The new data for 2008-2018 at HT revealed no significant change during the past decade in these air masses (p=0.83 to 0.85), suggesting that the ozone level in the outflow from eastern China may have reached or is reaching its peak. In Southeast Asia, previous analyses of vertical profiles from IAGOS aircraft and ozonesondes indicate an increase of about 20 ppbv in the boundary layer during summer from 1994-2004 to 2005-2014 (Gaudel et al. 2018). Our data suggest that the

effect of ozone precursors from Southeast Asia can be detected on the south China coast after the air masses have travelled over 1000 km (Figure 2a). We calculated the percentage contribution of each air group to the 'total ozone' at HT, which was calculated for each year as the average ozone value of the respective group multiplied by the number of trajectories in that group divided by the annual mean ozone multiplied by the total trajectories in that year. The largest contributor was the air mass from 'Eastern China' (41.0% ± 5.8%), followed by 'Aged continental' (30.6% ± 4.2%), 'Marine' (15.1% ± 3.6%) and 'Central China + PRD' (13.3% ± 2.8%) (Figure 2c). No significant trend was found in the transport pattern over the 25-year period.

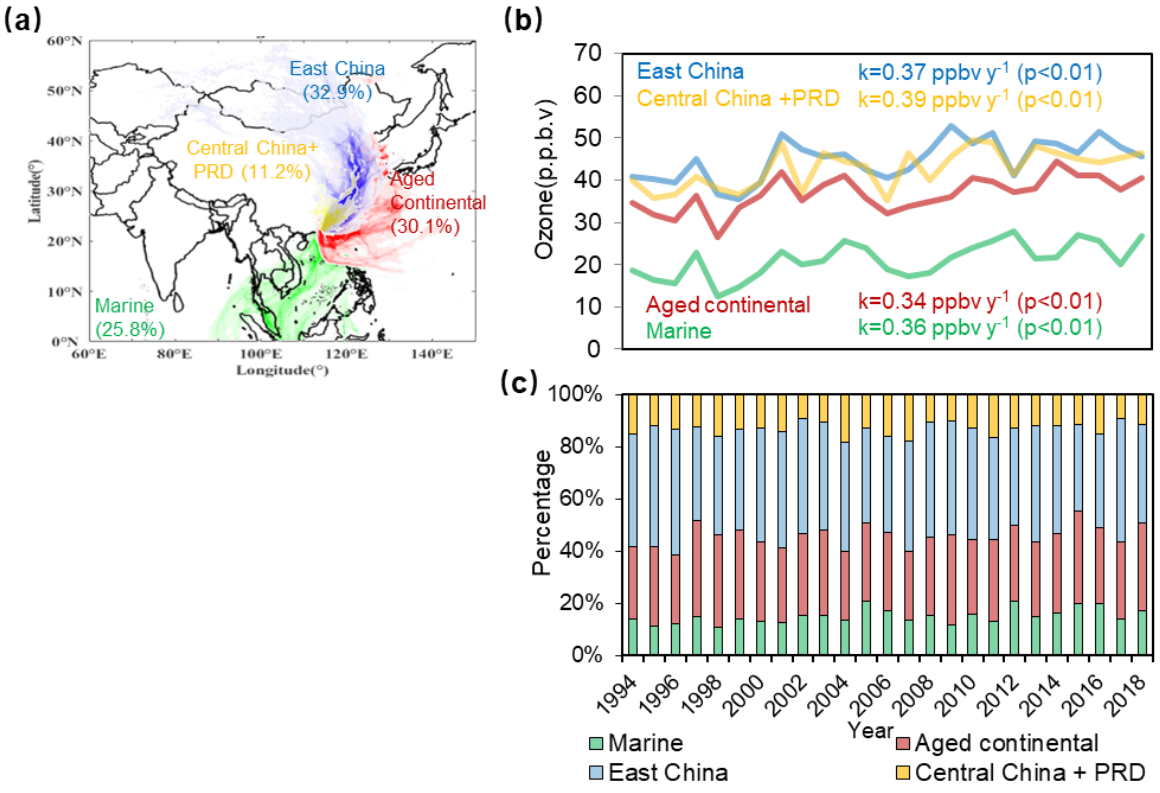

Figure 2. Surface ozone trend in four air-mass groups. (a) Spatial distribution of four types of 10-day hourly backward trajectories arriving at HT: 'East China' (blue), 'Aged continental' (red), 'Central China + PRD' (yellow) and 'Marine' (green). Percentage of each type during 1994-2018 is shown in parentheses. (b) Yearly mean ozone mixing ratios and linear fit results for each air mass group. (c) Percentage of contribution of each air-mass group to ozone budget at HT.

CO is emitted mainly from combustion processes from vehicles and biomass burning. Because it has a chemical lifetime of 1 to 2 months and does not dissolve in water, CO is an excellent tracer of anthropogenic emissions and an ozone precursor. The annual mean CO level at HT (Figure 3) appeared to decrease from 1994 to 2000, increased until 2006 and then decreased

again over the final 4 years. Seasonal and air-mass-segregated CO levels (Figure S2) showed overall negative trends in the continent-originated air masses (p=0.06 to 0.76) and a positive trend of 1.2 ppbv y^{-1} in the marine air mass (p=0.23). The CO data reveal opposite emission trends in the East Asia subcontinent and in subtropical Southeast Asia. We focus the remaining discussion on the drivers of the large increase seen in the maritime ozone.

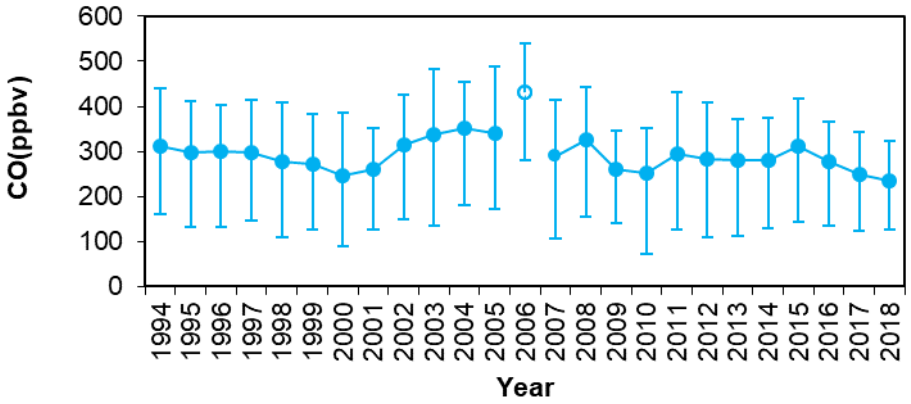

Figure 3. Long-term CO trend and variability in Hong Kong. Yearly mean CO mixing ratios (ppbv) at HT. Vertical bars indicate 75th and 25th percentiles. Data from March to September 2006 are not available due to instrument problems.

3.2. Impact of climate and emission in Southeast Asia on maritime ozone

We examined the NCEP meteorological data for the tropical and subtropical regions of East Asia (defined here as 0-25 °N and 100-120 °E, hereinafter referred to as Southeast Asia). The results reveal a dryer climate during the first part of the 25-year period (1994-2006), as indicated by the negative anomalies of specific humidity (-0.15±0.02 [$g.kg^{-1}$]) and rainfall (-1.03±0.02 [$kg.m^{-2}$]) and positive anomalies (0.12±0.07 [$g.kg^{-1}$] and 0.81±0.08 [$kg.m^{-2}$]) in the later period (2007-2018) (Figure 4a). Temperature and solar radiation, on the other hand, did not show a significant difference between the two periods (Figure 4b). On the ozone precursors, the satellite-derived column concentrations of nitrogen dioxide (NO_2) and formaldehyde (HCHO), a proxy of VOC emissions, for Southeast Asia show an increasing trend for both land and sea areas (p<0.01 to 0.05). These results suggest increasing emissions in NOx and VOCs in Southeast Asia including shipping activities in the South China Sea.

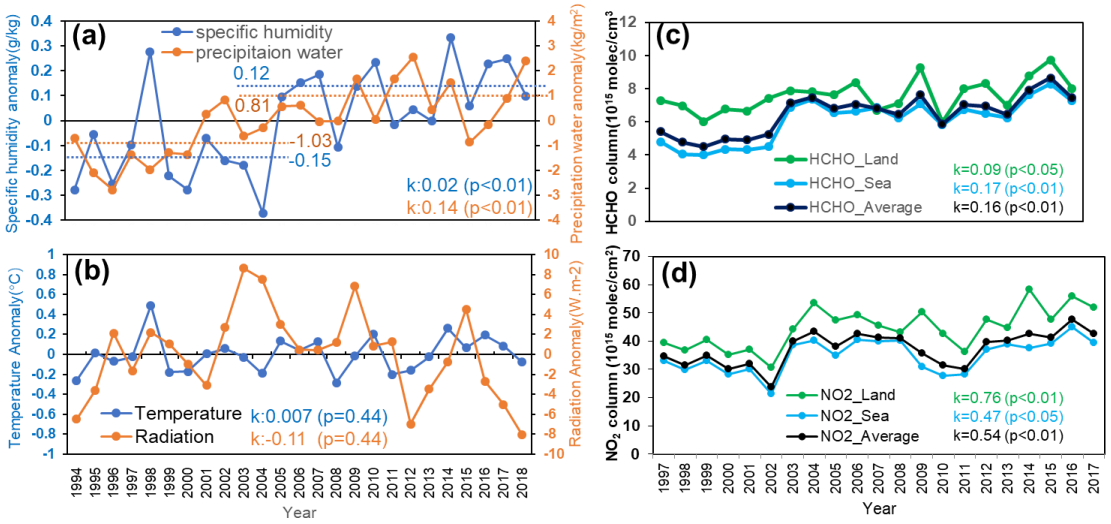

Figure 4. Long-term changes in meteorology and ozone precursors. Anomalies in NCEP data for Southeast Asia (including the South China Sea) for June-August from 1994-2018. (a) Specific humidity (g kg^{-1}) (blue, left axis) and precipitation (kg m^{-2}) (orange, right axis). (b) Temperature (°C) (blue, left axis) and radiation (Wm^{-2}) (orange, right axis). Dashed lines indicate the mean anomaly for period 1994-2006 and 2007-2018. (The 25-year mean: specific humidity:19.9 g kg^{-1}, precipitation: 48.6 kg m^{-2}, temperature: 27.4°C, radiation: 227 W m^{-2}). Yearly mean satellite observed column concentration of (c) NO_2 and (d) formaldehyde (10^{15} molec. cm^{-2}). Black, green and blue lines in c and d represent average value over whole domain, land and sea, respectively. Also shown are linear fit results.

We then evaluated the impact on summertime ozone by the apparent change in the climatic parameters in the early and later parts of the 25 years in Southeast Asia. We adopted the WRF-Chem model with updated nitrogen and chlorine chemistry and selected 3 months (July) from 1994-96 and from 2016-18 to represent typical summer conditions in the early years and in the recent years, respectively. Figure S3 shows the changes in the average values of the four parameters for the two three-summer periods. The emission data for 2016 are estimated from multiple sources. Model simulations of ozone in East Asia were performed with fixed emissions for each July of the 6 years (Fig S4), and Figure 5 shows the difference in the average July ozone level in the lowest 30-meter layer between the later and early years. The results indicate that the weather conditions in July 2016-2018 actually reduced ozone levels in Southeast Asia and southern China relative to July 1994-96. The more abundant water vapor in the early periods increased hydroxyl radicals (Figure S5), but the ozone production from HO_2+NO and RO_2+NO (Figure S6) decreased due to lower NO concentrations in Southeast Asia, which may be due to increase in atmospheric convections. Obviously, the changes in summer weather conditions in recent years cannot explain the observed increase in the maritime ozone level at our site, which is most likely due to increases in precursor emissions

from Southeast Asian countries and shipping activities in the South China Sea. Thus, we believe that the change in the regional climate has damped the effects of increased precursor emissions on the surface ozone levels in Southeast Asia. If the future weather condition reverts to the opposite phase (i.e. drier conditions), we would see a larger increase in maritime ozone if the precursor emissions in Southeast Asia are not reduced from their present levels.

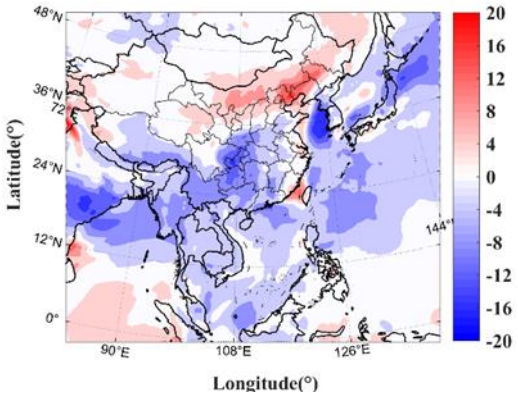

Figure 5. Sensitivity of summer surface ozone to meteorology in East Asia. Simulated ozone difference in the lowest 30-meter layer (Unit: ppbv) by WRF-Chem model in July from 2016 to 2018 and from 1994 to 1996**.**

4. Conclusion

We obtained the first long-term (>20 year) record of background ozone (and CO) levels in the subtropical part of East Asia, which fill in the data gap on the trend of these two trace gases and have significant relevance to air quality and climate. We find a sharp increase in the ozone level in maritime air masses influenced by the anthropogenic emissions from Southeast Asia and the slowing rate of increase in the continental air from China. Recent summer weather conditions may have masked the large impact of increasing emissions of ozone precursors in Southeast Asia. It is crucial to continue the long-term observations to detect possible decrease of ozone levels in China outflow (due to enhanced emission reductions in recent years) and future changes in maritime air from tropical and subtropical Asia. The increasing background ozone levels in air masses from both Northeast and Southeast Asia and in all seasons pose challenges to the mitigation of ground-level ozone pollution in Hong Kong and other coastal cities in south China. We suggest that regional cooperation is needed for air-quality improvement, not only among various cities in China but also including countries from Southeast Asia.

Acknowledgements. Funding for long-term measurements at Hok Tsui was provided by Hong Kong Polytechnic University (S-023). The data analysis in this work was supported by the

Hong Kong Research Grants Council (PolyU 153042/15E and T24-504/17-N). We thank Mike Anson, Lo-yin Chan, Y.S. Li and J.M. Ko for their contributions to the initiation and management of the Hok Tsui station in various periods of 1994-2018.

Author Contributions. T.W., K.S.L. and C.N.P. conducted the 25-year observations of O_3 and CO at Hok Tsui; T.W. designed the data analysis framework; J.N.D. processed the data, ran the model and made the plots; and T.W. wrote the paper with contributions from J.N.D. and G.P. B.

References

Akimoto, Hajime. 2003. 'Global air quality and pollution', *Science*, 302: 1716-19.

Boersma, KF, HJ Eskes, RJ Dirksen, JP Veefkind, P Stammes, V Huijnen, QL Kleipool, M Sneep, J Claas, and J Leitão. 2011. 'An improved tropospheric NO 2 column retrieval algorithm for the Ozone Monitoring Instrument', *Atmospheric Measurement Techniques*, 4: 1905-28.

Cooper, OR, DD Parrish, A Stohl, M Trainer, P Nédélec, V Thouret, Jean-Pierre Cammas, SJ Oltmans, BJ Johnson, and D Tarasick. 2010. 'Increasing springtime ozone mixing ratios in the free troposphere over western North America', *Nature*, 463: 344.

Council, National Research. 1992. *Rethinking the ozone problem in urban and regional air pollution* (National Academies Press).

De Smedt, I, J-F Müller, T Stavrakou, R Van Der A, H Eskes, and M Van Roozendael. 2008. 'Twelve years of global observations of formaldehyde in the troposphere using GOME and SCIAMACHY sensors', *Atmospheric Chemistry and Physics*, 8: 4947-63.

De Smedt, I, T Stavrakou, F Hendrick, T Danckaert, T Vlemmix, G Pinardi, N Theys, C Lerot, Clio Gielen, and C Vigouroux. 2015. 'Diurnal, seasonal and long-term variations of global formaldehyde columns inferred from combined OMI and GOME-2 observations', *Atmospheric Chemistry Physics Discussions*, 15: 12241–300.

De Smedt, I, M Van Roozendael, T Stavrakou, JF Müller, C Lerot, N Theys, P Valks, N Hao, and R Van Der A. 2012. 'Improved retrieval of global tropospheric formaldehyde columns from GOME-2/MetOp-A addressing noise reduction and instrumental degradation issues', *Atmos. Meas. Tech.*, 5: 2933-49.

Ding, AJ, Tao Wang, V Thouret, J Cammas, and P Nédélec. 2008. 'Tropospheric ozone climatology over Beijing: analysis of aircraft data from the MOZAIC program', *Atmospheric Chemistry Physics*, 8: 1-13.

Duncan, Bryan N, Lok N Lamsal, Anne M Thompson, Yasuko Yoshida, Zifeng Lu, David G Streets, Margaret M Hurwitz, and Kenneth E Pickering. 2016. 'A space-based, high-resolution view of notable changes in urban NOx pollution around the world (2005–2014)', *Journal of Geophysical Research: Atmospheres*, 121: 976-96.

Gaudel, Audrey, OR Cooper, Gérard Ancellet, Brice Barret, Anne Boynard, JP Burrows, Cathy Clerbaux, P-F Coheur, Juan Cuesta, and Emilio Cuevas Agulló. 2018. 'Tropospheric Ozone Assessment Report: Present-day distribution and trends of tropospheric ozone relevant to climate and global atmospheric chemistry model evaluation', *Elementa: Science of the Anthropocene*.

Grell, Georg A, Steven E Peckham, Rainer Schmitz, Stuart A McKeen, Gregory Frost, William C Skamarock, and Brian Eder. 2005. 'Fully coupled "online" chemistry within the WRF model', *Atmospheric Environment*, 39: 6957-75.

Jacob, Daniel J, Jennifer A Logan, and Prashant P Murti. 1999. 'Effect of rising Asian emissions on surface ozone in the United States', *Geophysical Research Letters*, 26: 2175-78.

Jacob, Daniel J, and Darrell A Winner. 2009. 'Effect of climate change on air quality', *Atmospheric Environment*, 43: 51-63.

Jaffe, Dan, Duli Chand, Will Hafner, Anthony Westerling, and Dominick %J Environmental science Spracklen. 2008. 'Influence of fires on O3 concentrations in the western US', *Environmental science technology*, 42: 5885-91.

Lefohn, Allen S, Christopher S Malley, Heather Simon, Benjamin Wells, Xiaobin Xu, Li Zhang, and Tao Wang. 2017. 'Responses of human health and vegetation exposure metrics to changes in ozone concentration distributions in the European Union, United States, and China', *Atmospheric Environment*, 152: 123-45.

Lin, Meiyun, Arlene M Fiore, Larry W Horowitz, Andrew O Langford, Samuel J Oltmans, David Tarasick, and Harald E Rieder. 2015. 'Climate variability modulates western US ozone air quality in spring via deep stratospheric intrusions', *Nature Communications*, 6: 7105.

Lin, Meiyun, Larry W Horowitz, Samuel J Oltmans, Arlene M Fiore, and Songmiao Fan. 2014. 'Tropospheric ozone trends at Mauna Loa Observatory tied to decadal climate variability', *Nature Geoscience*, 7: 136.

Lin, Meiyun, Larry W Horowitz, Richard Payton, Arlene M Fiore, and Gail Tonnesen. 2017. 'US surface ozone trends and extremes from 1980 to 2014: quantifying the roles of rising Asian emissions, domestic controls, wildfires, and climate', *Atmospheric Chemistry Physics*, 17.

Liu, Fei, Steffen Beirle, Qiang Zhang, Bo Zheng, Dan Tong, and Kebin He. 2017. 'NO x emission trends over Chinese cities estimated from OMI observations during 2005 to 2015', *Atmospheric Chemistry Physics*, 17: 9261-75.

Ma, Zhiqiang, Jing Xu, Weijun Quan, Ziyin Zhang, Weili Lin, and Xiaobin Xu. 2016. 'Significant increase of surface ozone at a rural site, north of eastern China', *Atmospheric Chemistry Physics*, 16: 3969-77.

Mann, Henry B. 1945. 'Nonparametric tests against trend', *Econometrica: Journal of the Econometric Society*: 245-59.

Monks, Paul Steven, AT Archibald, Augustin Colette, O Cooper, M Coyle, R Derwent, D Fowler, Claire Granier, Kathy S Law, and GE %J Atmospheric Chemistry Mills. 2015. 'Tropospheric ozone and its precursors from the urban to the global scale from air quality to short-lived climate forcer', *Atmospheric Chemistry Physics*, 15: 8889-973.

Neu, Jessica L, Thomas Flury, Gloria L Manney, Michelle L Santee, Nathaniel J Livesey, and John Worden. 2014. 'Tropospheric ozone variations governed by changes in stratospheric circulation', *Nature Geoscience*, 7: 340.

Okamoto, S, H Tanimoto, N Hirota, K Ikeda, and H Akimoto. 2018. 'Decadal Shifts in Wind Patterns Reduced Continental Outflow and Suppressed Ozone Trend in the 2010s in the Lower Troposphere Over Japan', *Journal of Geophysical Research: Atmospheres*, 123: 12,980-12,93.

Pachauri, RK, L Meyer, GK Plattner, and T Stocker. 2014. 'IPCC, 2014: climate change 2014: synthesis report', *IPCC*.

Parrish, DD, J‐F Lamarque, V Naik, L Horowitz, DT Shindell, J Staehelin, R Derwent, OR Cooper, H Tanimoto, and A Volz‐Thomas. 2014. 'Long‐term changes in lower tropospheric baseline ozone concentrations: Comparing chemistry‐climate models and observations at northern midlatitudes', *Journal of Geophysical Research: Atmospheres*, 119: 5719-36.

Sen, Pranab Kumar 1968. 'Estimates of the regression coefficient based on Kendall's tau', *Journal of the American statistical association*, 63: 1379-89.

Sun, Lei, Likun Xue, Tao Wang, Jian Gao, Aijun Ding, Owen R Cooper, Meiyun Lin, Pengju Xu, Zhe Wang, and Xinfeng Wang. 2016. 'Significant increase of summertime ozone at Mount Tai in Central Eastern China', *Atmospheric Chemistry Physics*, 16: 10637-50.

Wang, Tao, XL Wei, AJ Ding, Steven CN Poon, KS Lam, YS Li, LY Chan, and Michael Anson. 2009. 'Increasing surface ozone concentrations in the background atmosphere of Southern China, 1994-2007', *Atmospheric Chemistry Physics*, 9: 6217-27.

Warneck, Peter. 1999. *Chemistry of the natural atmosphere*.

Wasserstein, Ronald L, Allen L Schirm, and Nicole A Lazar. 2019. "Moving to a World Beyond “p< 0.05”." In.: Taylor & Francis.

Westerling, Anthony L, Hugo G Hidalgo, Daniel R Cayan, and Thomas W %J science Swetnam. 2006. 'Warming and earlier spring increase western US forest wildfire activity', 313: 940-43.

Zhang, Li, QY Li, Tao Wang, Ravan Ahmadov, Qiang Zhang, Meng Li, and MY Lv. 2017. 'Combined impacts of nitrous acid and nitryl chloride on lower-tropospheric ozone: new module development in WRF-Chem and application to China', *Atmospheric Chemistry Physics*, 17: 9733-50.

Zhang, Yuqiang, Owen R Cooper, Audrey Gaudel, Anne M Thompson, Philippe Nédélec, Shin-Ya Ogino, and J Jason West. 2016. 'Tropospheric ozone change from 1980 to 2010 dominated by equatorward redistribution of emissions', *Nature Geoscience*, 9: 875.

Supporting Information

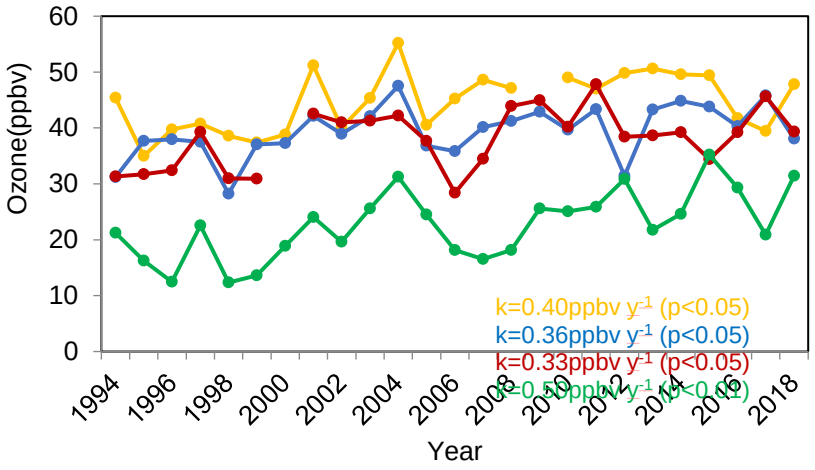

Figure S1. Trend in seasonal O_3 during 1994-2018.

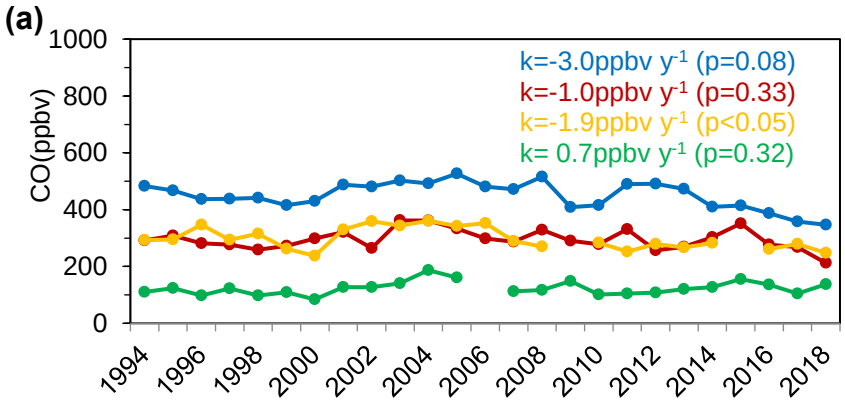

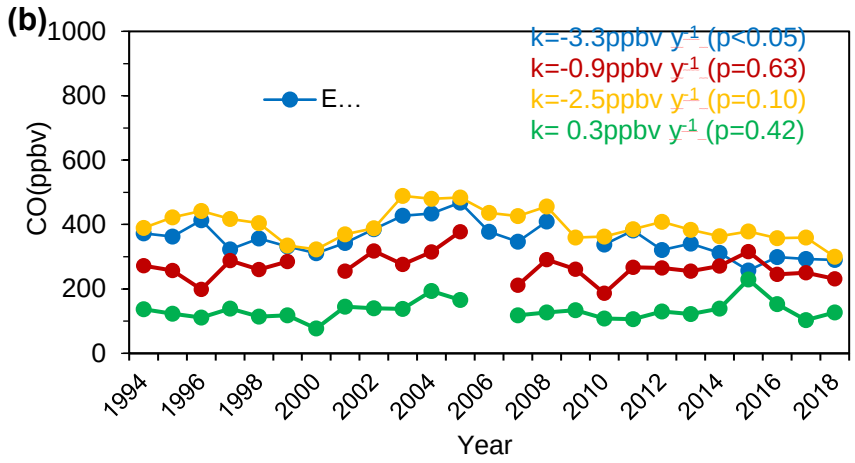

Figure S2. Trend in (a)seasonal and (b)air-mass segregated CO during 1994-2018.

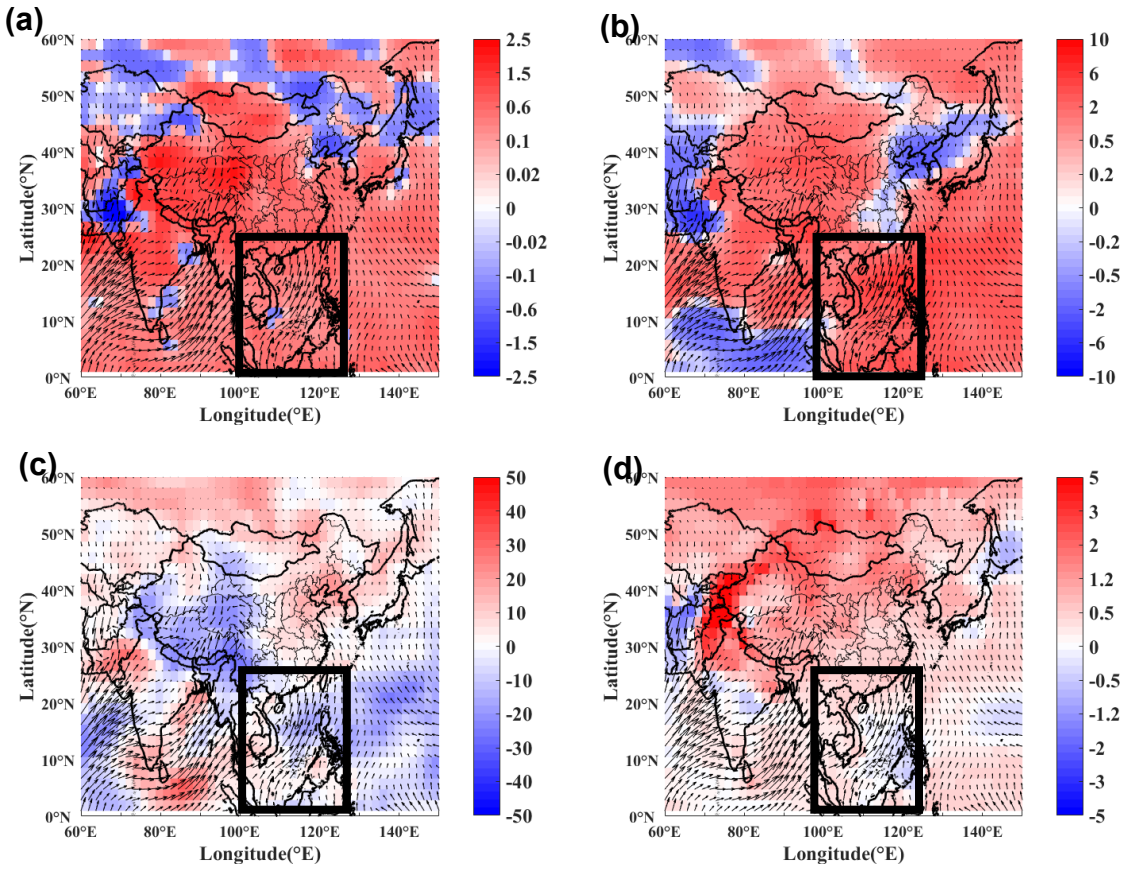

Figure S3. Spatial distribution of difference in NCEP/NCAR meteorological parameters between July in 2016-18 and 1994-16. (a) Specific humidity (g.kg^{-1}), (b) precipitation (kg.m^{-2}), (c) radiation (W.m^{-2}), (d) temperature (°C). Black arrows represent wind direction at 10-m height in July 2016-18. Black box shows Southeast Asia including the South China Sea (0-25 °N; 100 -120 °E).

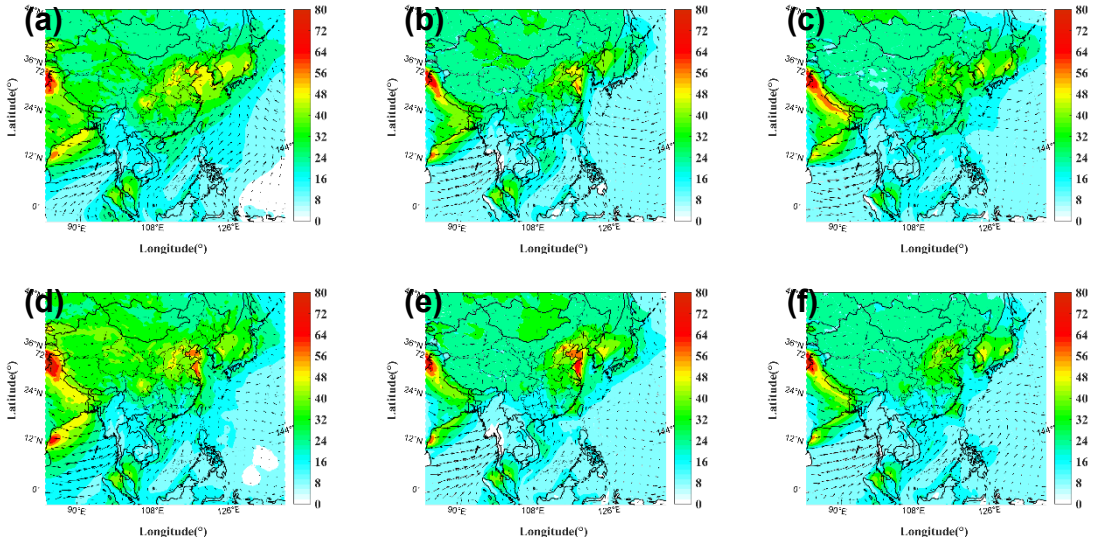

Figure S4. Simulated spatial distribution of surface ozone in the lowest 30-meter layer (ppbv) in July (a) 1994, (b) 1995, (c) 1996, (d) 2016, (e) 2017 and (f) 2018. Black arrows represent the wind vector at 10-m height in July.

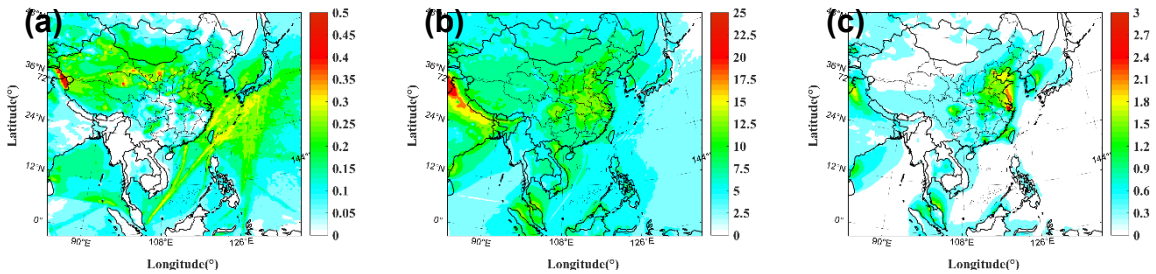

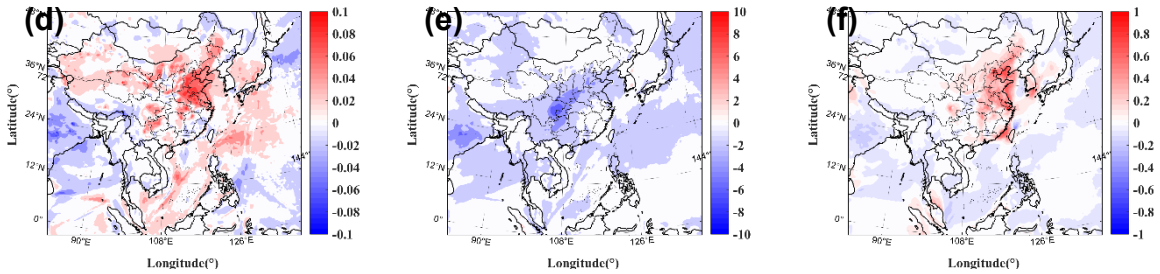

436

437 Figure S5. Simulated spatial distribution of (a) OH, (b) HO_2 and (c) RO_2 (in July 2016-18)
438 (pptv) and difference between respective values in July 1994-96 and July 2016-18 (e), (f) and
439 (g) in the lowest 30-meter layer with 2016 emission.

440

441

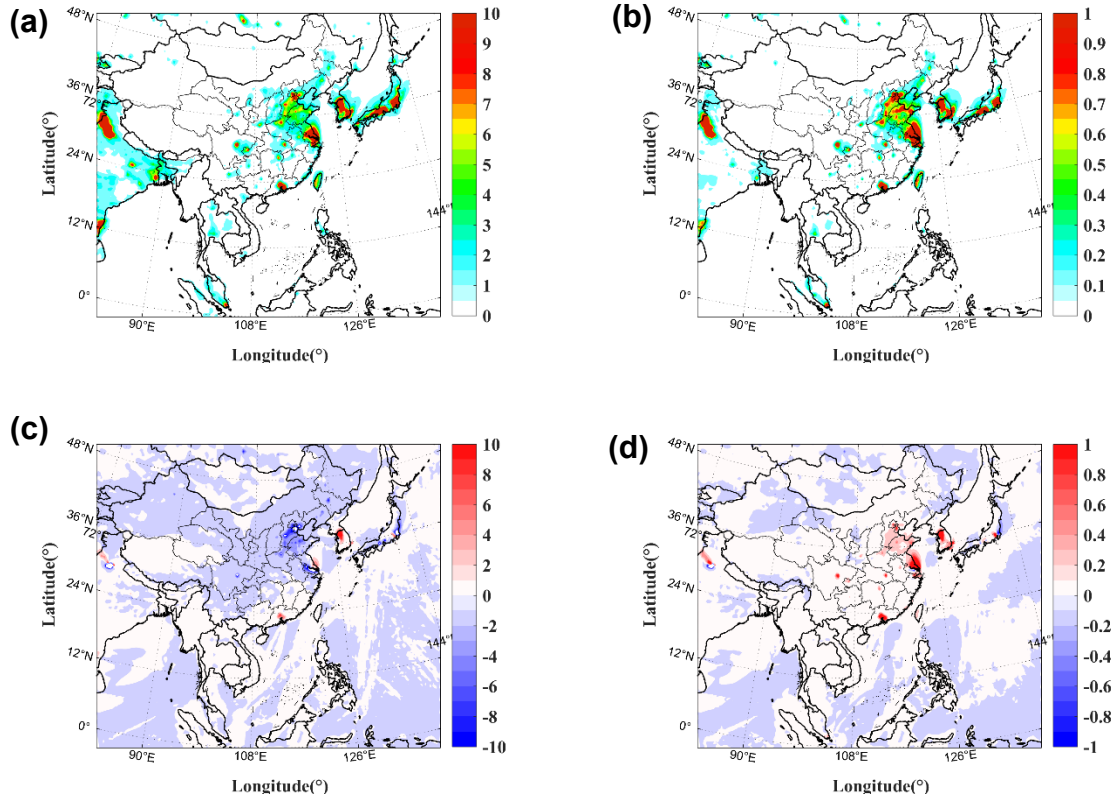

442

443 Figure S6. Simulated spatial distribution of (a) $k_1[HO_2]$ [NO] and (b) $k_2[RO_2]$ [NO] (in July
444 2016-18) (ppbv h^{-1}) and difference between the respective values in the lowest 30-meter layer
445 in July 2016-18 and 1994-96 (c), (d).

446

447